Journal of Physics: Condensed Matter

Energy and momentum relaxation of hot electrons in GaN/AlGaN

To cite this article: N Balkan *et al* 2002 *J. Phys.: Condens. Matter* **14** 3457

View the article online for updates and enhancements.

Related content

- Effect of non-drifting hot phonons on high-field drift velocity in GaN/AlGaN
  S Gokden, N Balkan and B K Ridley
- Hot electron cooling rates via the emission of LO-phonons in InN
  D Zanato, N Balkan, B K Ridley et al.
- Hot-electron energy relaxation rates in GaAs/GaAlAs quantum wells
  N Balkan, B K Ridley, M Emeny et al.

Recent citations

- Quantum coupling and electrothermal effects on electron transport in high-electron mobility transistors
  Ling-Feng Mao
- Current Reduction Caused by the Quantum Coupling of Hot Electrons in AlGaN/GaN Transistors
  Ling-Feng Mao
- Negative Differential Resistance Observation and a New Fitting Model for Electron Drift Velocity in GaN-Based Heterostructures
  Gokhan Atmaca *et al*

IOP ebooks™

Bringing you innovative digital publishing with leading voices to create your essential collection of books in STEM research.

Start exploring the collection - download the first chapter of every title for free.

This content was downloaded from IP address 193.255.189.6 on 28/08/2019 at 14:09

INSTITUTE OF PHYSICS PUBLISHING JOURNAL OF PHYSICS: CONDENSED MATTER

J. Phys.: Condens. Matter **14** (2002) 3457–3468 PII: S0953-8984(02)28578-1

Energy and momentum relaxation of hot electrons in GaN/AlGaN

N Balkan[1,5], M C Arikan[2], S Gokden[3], V Tilak[4], B Schaff[4] and R J Shealy[4]

[1] University of Essex, Department of Electronic Systems Engineering, Colchester, UK
[2] University of Istanbul, Department of Physics, Vezneciler, Istanbul, Turkey
[3] Balikesir University, Department of Physics, Balikesir, Turkey
[4] Cornell University, Department of Electrical and Computing Engineering, Ithaca, NY, USA

E-mail: balkan@essex.ac.uk

Received 6 September 2001, in final form 18 December 2001
Published 22 March 2002
Online at stacks.iop.org/JPhysCM/14/3457

Abstract

We report the experimental studies of hot-electron energy and momentum relaxation in the steady state in GaN/AlGaN HEMT structures with a high two-dimensional electron density of $n = 1.5 \times 10^{13}$ cm^{-2}. From the LO-phonon-scattering-limited component of the mobility we obtain for the LO phonon the energy of $\hbar\omega \sim 90$ meV and the momentum relaxation time of $\tau_m \sim 4$ fs. Drift velocity versus electric field characteristics obtained from the pulsed I–V measurements show that, at $T_L = 77$ K, the drift velocity saturates at $v_d = 1.0 \times 10^7$ cm s^{-1} at electric fields in excess of $E \sim 7.5$ kV cm^{-1}, and at $T_L = 300$ K it saturates at $v_d \sim 5 \times 10^6$ cm s^{-1}, at an electric field of around $E \sim 10$ kV cm^{-1}. Electron temperature as a function of applied electric field is obtained by comparing the measured electric field dependence of the mobility μ_E at a fixed lattice temperature, with the lattice temperature dependence of the mobility at a fixed low electric field. The electron energy loss rate is then determined from the electron temperature dependence of the power loss using the power balance equations. The effect of hot-phonon production on the observed momentum and energy relaxation of hot electrons is discussed within the framework of a theoretical model, which was originally developed for III–V material systems and has been adapted for a two-dimensional electron gas in GaN, and in which phonon drift is neglected.

1. Introduction

The wide-bandgap III nitride semiconductors have found many applications in optoelectronic and electronic device technologies. They are ideal structures for LEDs and lasers, for

[5] Author to whom any correspondence should be addressed.

© 2002 IOP Publishing Ltd Printed in the UK

applications in displays and high-density data storage respectively, as well as high-power FETs operating at high temperatures [1–3]. Compared with their technological applications, fundamental research in nitrides appears to be still in its infancy. Until recently, the poor material quality was partly responsible for the slow progress in experimental research. For example measurements of electron effective mass, electron acoustic and optic phonon scattering rates and determination of quantum mobility have been reported only very recently [4–6]. Very little experimental work has been done at high electric fields. In bulk GaN, for example, there have been only a few reports concerning energy relaxation of hot electrons using electrical [7] and optical techniques [9], and very limited results concerning high-field momentum relaxation [10]. Theoretical and Monte Carlo calculations predict very high drift velocities [11, 12]. High-speed measurements appear to support these predictions [13]. In GaN/AlGaN, however, to our knowledge there is no reported work concerning the energy and momentum relaxation measurements in the steady state. The interest in the high-field applications on GaN/AlGaN HEMT structures makes it vital to obtain a detailed understanding of the transport properties at high fields. The determination of the dominant scattering mechanisms and the limitations these might impose on device performance are very important. The current work aims to measure, in the steady state, the energy and momentum relaxation of a high density of two-dimensional electrons formed as a result of spontaneous and piezoelectric polarization at the GaN/AlGaN interface, and compare the results with existing theories.

2. Experimental results and discussions

2.1. Hall measurements

The samples investigated in this work were grown using MBE on tungsten-backed sapphire substrates. Tungsten is evaporated onto the sapphire to act as a heat sink to dissipate excess thermal energy at high electric fields. The thickness of the GaN buffer layer is 3 μm, and the Al concentration of the 250 Å thick GaAlN layer is 30% as determined from PL measurements. Hall measurements were carried out using a Van der Pauw geometry. For pulsed I–V measurements a simple bar sample with length l and width w ($l = w = 1$ mm) was used. Indium was annealed onto both samples to provide ohmic contacts. Hall measurements were performed at temperatures between $T_L = 4.2$ and 300 K using a variable temperature cryostat and an electromagnet assembly. A stable constant current supply was used in the measurements. Current supply through the sample was deliberately kept low to ensure ohmic conditions, hence the two-dimensional electrons were in thermal equilibrium with the lattice. Both the carrier density and Hall mobility were independent of current and magnetic field at all temperatures for injected currents between $I = 1.0$ μA and 30 mA and for magnetic fields between $B = 0.35$ and 3 T. Figure 1 shows the two-dimensional carrier density and Hall mobility between $T_L = 4.2$ and 300 K. The two-dimensional electron density at $T_L = 4.2$ K is $n = 1.5 \times 10^{13}$ cm^{-2}. It remains constant up to $T_L = 150$ K then increases rapidly to $n = 2.1 \times 10^{13}$ cm^{-2} at $T_L = 300$ K. The high density of electrons is due to large spontaneous and strain-induced polarization in the GaN/AlGaN interface as commonly predicted and observed [14]. The increase in the carrier density at high temperature is due to parallel conduction in the AlGaN layer. At $T = 4.2$ K the Hall mobility is $\mu = 2830$ cm^2 V^{-1} s^{-1}. It decreases very little (by 3%) with temperature up to $T_L = 80$ K, then decreases rapidly down to $\mu = 743$ cm^2 V^{-1} s^{-1} at $T = 300$ K. At high temperatures the measured Hall mobility will contribute due to the finite parallel conductivity in the GaAlN layer according to [15]

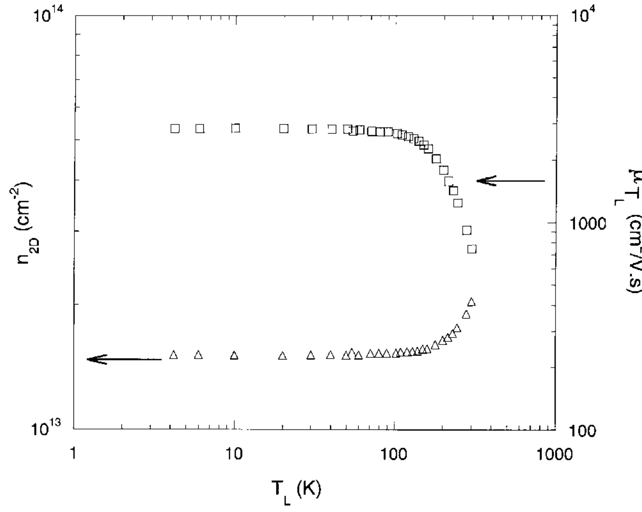

Figure 1. Two-dimensional electron density and Hall mobility versus temperature.

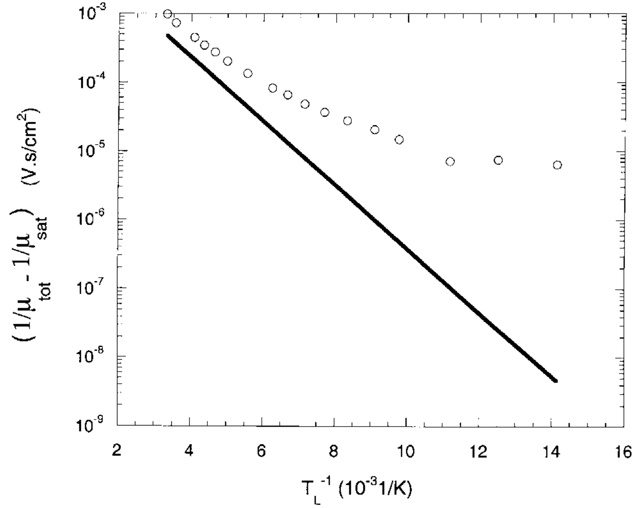

Figure 2. Logarithm of the inverse of the LO-phonon-limited mobility versus inverse lattice temperature. Open circles: experimental results, obtained from the measured Hall mobility versus temperature data using Matthiessen's rule. Line: theoretical calculation using equation (4).

$$n_H = \frac{n_1\mu_1 + n_2\mu_2}{\mu_H} \tag{1}$$

$$\mu_H = \frac{n_1\mu_1^2 + n_2\mu_2^2}{n_1\mu_1 + n_2\mu_2} \tag{2}$$

where n_H and μ_H are the measured Hall carrier density and Hall mobility and n_1, n_2, μ_1 and μ_2 are the two-dimensional carrier density in GaN, sheet density in AlGaN and electron mobilities in GaN and AlGaN, respectively. If we take $n_1 = n_H$ ($T = 4.2$ K) and $\mu_1 = 1000$ cm^2 V^{-1} s^{-1} (LO-phonon-limited mobility, see figure 2) using the n_H and μ_H values measured at $T_L = 300$ K in equation (1) we find $n_2\mu_2 \approx 0.05 n_1\mu_1$. Furthermore, the

mobility of three-dimensional electrons in the GaAlN is expected to be low compared with that of the two-dimensional electron gas in GaN [16]. We can assume, therefore, that in equation (2), $\mu_H \approx \mu_1$ with an accuracy of around $\pm 10\%$, and the measured μ_H is representative of the two-dimensional electrons at the interface. At high temperatures μ_1 is primarily determined by e–LO phonon scattering [17]. We can, therefore, use Matthiessen's rule to separate the LO-phonon-scattering-limited component of the mobility via

$$\frac{1}{\mu_{LO}} = \frac{1}{\mu_{tot}} - \frac{1}{\mu_0} \tag{3}$$

where μ_0 is the low-temperature mobility and μ_{tot} is the measured temperature-dependent mobility ($\mu_{tot} = \mu_H$). In figure 2 the logarithm of $(1/\mu_{LO})$ determined from the experimental results is plotted against $1/T_L$. We have also plotted a theoretical LO-phonon-limited mobility in the form

$$\frac{1}{\mu_{LO}} = \frac{m^*}{e\tau_m} \exp\left(\frac{-\hbar\omega}{kT_L}\right) \tag{4}$$

where $m^* = 0.22\ m_0$, $\hbar\omega = 92$ meV. In the plot we took momentum relaxation time, τ_m as the electron phonon scattering time constant, $\tau_0 = 8 \times 10^{-15}$ s. In the high-temperature region ($T > 180$ K) experimental data develop an exponential dependence, as in equation (4). In this region, from the slope of $\log\left(\frac{1}{\mu_{tot}} - \frac{1}{\mu_{sat}}\right)$ we obtain $\hbar\omega = 90$ meV. This is in good agreement with the theoretical value. However, at 300 K the magnitude of the experimental data is about a factor of two higher than that in equation (4). This suggests a momentum relaxation time of $\tau_m = \tau_0/2 = 4 \times 10^{-15}$ s, a value much smaller than the theoretically expected electron momentum relaxation time [17] but in accord with other observations [18–20]. The reason for the reduced momentum relaxation time and hence mobility compared with the theory is not clear to us. Interface roughness scattering is often invoked as the cause of reduced mobility in GaN/GaAlN [16]. For example for a two-dimensional electron density of $n = 1.0 \times 10^{13}$ cm^{-2}, an interface roughness of thickness 5 Å and width 50 Å is shown to reduce the room-temperature mobility by about a factor of two, compared with the LO-limited mobility [16]. However our observation in figure 2, which excludes all scattering mechanisms, that are either temperature independent or slowly varying functions of temperature, cannot be explained in terms of interface roughness scattering.

2.2. *High-field drift velocity*

For the high-speed I–V measurements we used a simple bar of length $l = 1$ mm and width $w = 1$ mm, fabricated using the section of the wafer where the Van der Pauw measurements were made. I–V characteristics were measured at lattice temperatures $T_L = 77$ and 300 K. In these measurements, voltage pulses of 300 ns duration (or less at higher fields), with a duty cycle of better than 3×10^{-4}, were applied along the length of the sample up to a maximum electric field of $E = 10^4$ V cm^{-1}. Both the applied voltage and current through the sample were measured using a 1 GHz real time oscilloscope. Drift velocity (v_d) versus electric (E) field is obtained, directly, from the pulsed I–V characteristics assuming that the free carrier density is not a function of applied electric field [21]. Figure 3 shows the pulsed I–V plot measured at $T_L = 77$ K. The resistance is ohmic at applied voltages $V < 120$ V ($E < 1200$ V cm^{-1}). At higher voltages the I–V characteristic becomes non-linear, as would be expected from increased momentum scattering of hot electrons with LO phonons. At high voltages ($V > 750$ V), the current saturates at $I \approx 620$ mA. In the v_d–E plot in figure 4 this saturation corresponds to a drift velocity of around $v_d = 1.0 \times 10^7$ cm s^{-1} at an electric field of $E = 7500$ V cm^{-1}. To our knowledge, this is the first reported drift velocity-field measurement

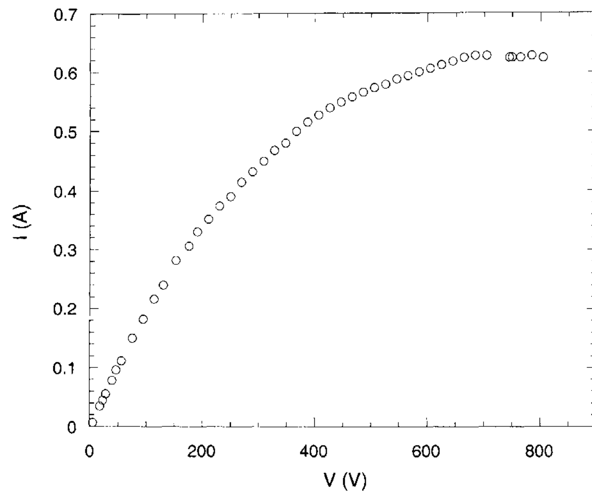

Figure 3. Pulsed current–voltage measurements at lattice temperature, $T_L = 77$ K.

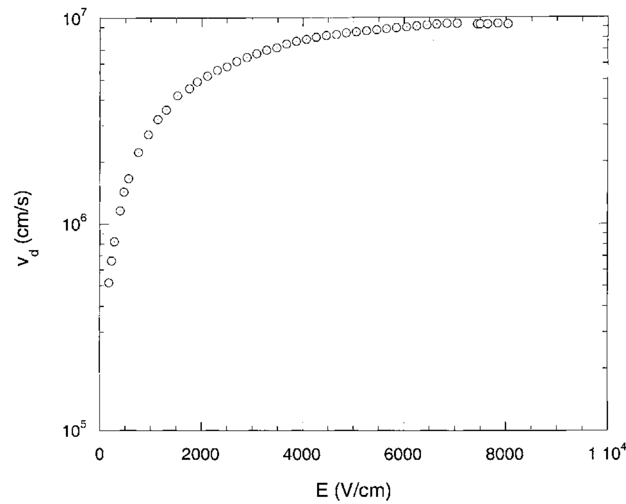

Figure 4. Logarithm of electron drift velocity versus applied electric field measured at lattice temperature, $T_L = 77$ K.

in the steady state in GaN/AlGaN. It is clear that the highest attainable drift velocity in the steady state is much smaller than the peak velocities predicted by theory, Monte Carlo simulation and those measured in the transient mode in the picosecond time domain [11–13, 22]. The reason for the reduced drift velocity might be associated with the production of non-equilibrium (hot) phonons at high fields. If hot phonons share the drift of electrons, re-absorption of these by electrons does not affect the momentum relaxation. However, the phonon scattering by imperfections (interface roughness, dislocations etc) during the lifetime of hot phonons ($\tau = 5$ ps) [6] reduces the phonon drift significantly. Thus electron momentum relaxation rate is expected to increase, similar to our earlier observations in GaAs/GaAlAs MQWs, where the non-equilibrium phonon drift was demonstrated to decrease due to their elastic scattering from interface roughness [23–25].

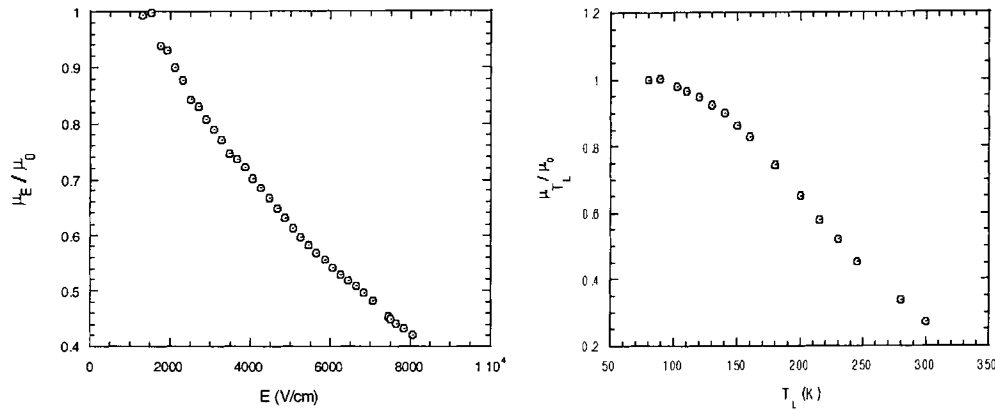

Figure 5. Field-dependent electron mobility at lattice temperature, $T_L = 77$ K normalized with respect to the ohmic mobility, and the temperature-dependent mobility normalized with respect to the ohmic mobility.

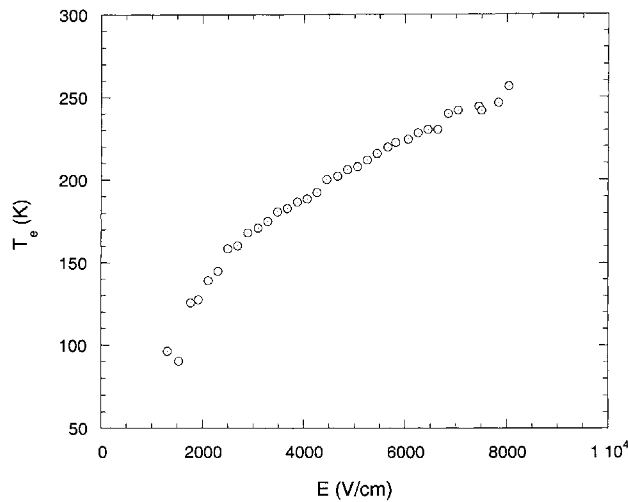

Figure 6. Electron temperature versus applied electric field at lattice temperature of $T_L = 77$ K obtained by comparing the normalized mobility curves in figure 5.

2.3. Hot-electron energy loss rates

The technique used in this work to obtain the temperature of the non-equilibrium electrons is known as the 'mobility comparison' method. The method has been used successfully in two-dimensional GaAs [23, 24] and bulk GaN [7, 10] and involves the measurement of both the electric field dependence of the mobility (μ_E) at a fixed lattice temperature, and the lattice temperature dependence of the mobility at a fixed low electric field. The two sets of results are then normalized with respect to low-field mobility and low-temperature mobility respectively. Plots of the normalized mobility values against lattice temperature and electric field are shown in figure 5, where the base lattice temperature is $T_L = 77$ K. Electron temperature as a function of electric field obtained by comparing the two plots is shown in figure 6. Electron temperature rises above the lattice temperature at electric fields of around $E \approx 1200\ \mathrm{V\ cm^{-1}}$. The maximum

electron temperature reached in the experiments at $E = 8$ kV cm^{-1} is $T_e = 260$ K. It should be noted that the accuracy of the mobility comparison method *strictly* assumes that

(1) the carrier density does not change with field;
(2) e–e scattering rate thermalizes the hot electrons amongst themselves, hence the non-equilibrium electron distribution can be represented by an electron temperature which is greater than the lattice temperature;
(3) the dependence of momentum relaxation on electron temperature (electric field) is identical to its dependence on lattice temperature. The variation of the low-field mobility with lattice temperature, in the LO phonon regime, involves the emission and absorption of LO phonons randomly distributed in the $\boldsymbol{k}$ space, with both the electrons and phonons in thermal equilibrium with the lattice, i.e. $T_e = T_p = T_L$ (T_p is the 'phonon' temperature). Therefore the following conditions must hold:
    (i) at high fields non-equilibrium phonons must exist;
    (ii) the characteristic temperature of the hot phonons must be close to the electron temperature and
    (iii) the hot-phonon distribution at high fields should be randomized in $\boldsymbol{k}$ space, as it is at low fields.

If any of these conditions are not satisfied electron temperatures and hence energy relaxation rates obtained from the mobility comparison experiment will be wrong.

In order to calculate the energy loss rates from the experimental results we used the power balance equations. In the steady state the input power (p) is equal to the power loss ($\mathrm{d}E/\mathrm{d}T$) to the lattice through scattering processes. Therefore, the energy loss rate per electron can be obtained as a function of electric field via

$$p = e\mu_E E^2 = \mathrm{d}E/\mathrm{d}T \tag{5}$$

where μ_E is the mobility at electric field E. The power loss per electron can also be obtained as a function of electron temperature using equation (5) together with figure 6. This is shown in figure 7, where the logarithm of the power input (loss) per electron (p) is plotted versus inverse electron temperature ($1/T_E$) at a lattice temperature $T_L = 77$ K. Also shown in the figure is the power loss involving the emission and absorption of LO phonons at $T_L = 77$ K in the form

$$\begin{aligned} \mathrm{d}E/\mathrm{d}T = p &= \frac{\hbar\omega}{\tau_0}\left[\exp\left(\frac{-\hbar\omega}{kT_E}\right) - \exp\left(\frac{-\hbar\omega}{kT_L}\right)\right] \\ \tau_0 &= \left[\frac{e^2\omega}{2\pi\hbar}\left(\frac{m^*}{2\hbar\omega}\right)^{1/2}\left(\frac{1}{\varepsilon_\infty} - \frac{1}{\varepsilon_s}\right)\right]^{-1} \end{aligned} \tag{6}$$

where ε_∞, ε_s, τ_0 are high-frequency and static permittivities and the time constant for e–LO phonon scattering respectively. Taking for GaN $m^*/m_0 = 0.22$, $\varepsilon_\infty/\varepsilon_0 = 5.35$, $\varepsilon_s/\varepsilon_0 = 9.7$ and the e–LO phonon energy $\hbar\omega = 92$ meV, we find the scattering time $\tau_0 = 8$ fs.

It is clear from figure 7 that the observed power loss has a slope which is much smaller than the theoretical power loss, described by equation (6). The slope decreases with decreasing temperature, indicating the prevalence of lower-energy (acoustic) phonons in the energy loss with a non-exponential temperature [7, 8, 10]. It is evident from the lattice temperature dependence of the electron mobility (figure 2) that there is a considerable momentum scattering by LO phonons at lattice temperatures around $T_L \sim 160$ K. Therefore at electron temperatures of $T_E > 160$ K optic phonon scattering should also be the dominant energy loss mechanism. Figure 7 indicates, however, that only in a very small range of electron temperature (160–190 K) is the slope of the power loss close to the line representing the theoretical loss in equation (6).

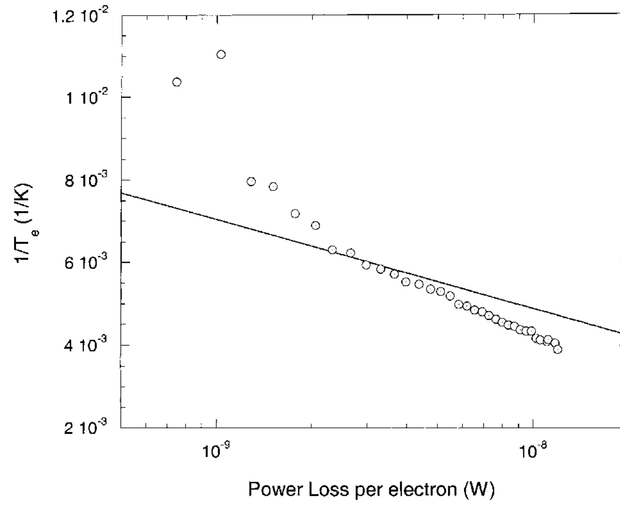

Figure 7. Circles: logarithm of experimental power loss per electron versus inverse electron temperature. Line: theoretical power loss obtained from equation (6).

At temperatures $T_E > 190$ K the experimental loss rate is gradually reduced compared with the theory. This behaviour would be expected if the free carrier density were reduced by increasing field [21], or if there were hot phonons present at high fields. One of the assumptions made in the mobility comparison method is the presence of non-equilibrium phonons. If this assumption is correct the magnitude of the experimental loss rate obtained from the mobility comparison method should, indeed, deviate from the theoretical line represented by equation (6), which does not include the hot-phonon effects. In order to calculate the effect of hot-phonon production on the energy relaxation rates, we have adapted the non-equilibrium phonon model, developed for two-dimensional and bulk GaAs by Ridley [25], to the case of two-dimensional GaN. In the model the power loss is given by

$$\mathrm{d}E/\mathrm{d}T = p = \frac{\hbar\omega}{\tau_{eff}}\left[\exp\left(\frac{-\hbar\omega}{kT_E}\right) - \exp\left(\frac{-\hbar\omega}{kT_L}\right)\right]. \tag{7}$$

This equation is similar to equation (6). However, the e–LO phonon scattering time constant τ_0 is replaced by the effective energy relaxation time, τ_{eff}, which takes into account all the hot-phonon effects. For intrasubband scattering in a deep quantum well via the interaction LO phonons in the non-degenerate case the effective energy relaxation time [25]

$$\tau_{eff} = \tau_{02D}(1+\gamma) \tag{8}$$

where τ_{02D} is the characteristic scattering time in the QW, namely,

$$\tau_{02D} = \tau_0\left(\frac{\hbar\omega}{E_L}\right)^{1/2} \qquad E_L = \frac{\hbar^2\pi^2}{2m^*L^2} \tag{9}$$

and

$$\gamma = \frac{\tau_p}{2\tau_0}\frac{1}{q_0L}\left(\frac{\pi k_BT_E}{\hbar\omega}\right)^{1/2}\frac{n}{N_c}\left[1-\exp\left(-\frac{\hbar\omega}{k_BT_E}\right)\right] \qquad q_0 = \left(\frac{2m^*\omega}{\hbar}\right)^{1/2} N_c = \frac{m^*k_BT_E}{\pi\hbar^2L} \tag{10}$$

where q_0, L, τ_p, n and N_c are the phase matching wave vector, well width, phonon lifetime, three-dimensional electron density ($n = n_{2D}/L$) and the effective density of states respectively.

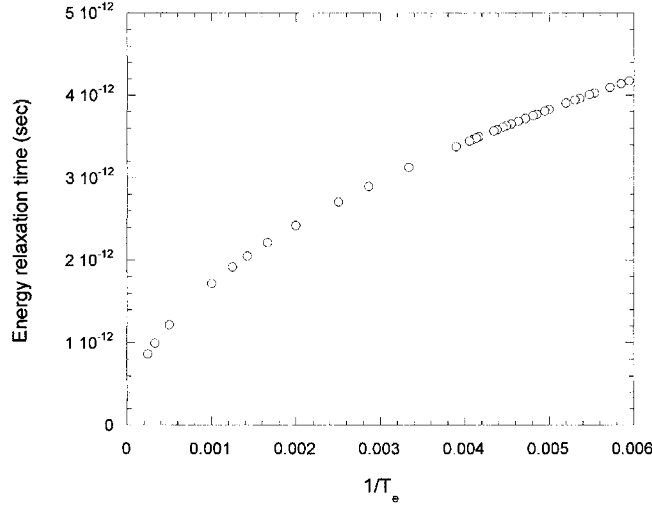

Figure 8. Effective energy relaxation time versus inverse electron temperature, calculated for $n_{2D} = 1.5 \times 10^{13}$ cm^{-2}, at $T_L = 77$ K, using equations (7)–(10) in the degenerate regime.

In the calculations of τ_{eff} we used the following parameters: $m^* = 0.22m_0$, $\tau_p = 5$ ps, $n_{2D} = 1.5 \times 10^{13}$ cm^{-2}, $\hbar\omega = 92$ meV, $\varepsilon_\infty = 9.7\varepsilon_0$, $\varepsilon_s = 5.35\varepsilon_0$, $\tau_0 = 8$ fs, $q_0 = 7.3 \times 10^8$ m^{-1}.

We assumed that the effective well width of the potential well at the GaN/AlGaN interface is

$$L \approx \lambda_F = 65 \text{ Å}$$

where λ_F is the Fermi wavelength corresponding to a Fermi level of

$$E_F = \frac{nh^2}{4\pi m^*} = 163 \text{ meV}.$$

For simplicity, we have also assumed that, at high fields, $\hbar\omega/E_L \approx 1$ and therefore, $\tau_{02D} = \tau_0$.

τ_{eff} versus $1/T_E$ calculated using equations (7)–(10), is plotted in figure 8. As a result of the high effective density of states the non-degenerate condition is expected to be reached at very high electron temperatures where the effective energy relaxation time depends on the electron temperature and, therefore, on the electric field. We have also calculated the effective energy relaxation time constant τ_{eff} for the degenerate case, because the highest electron temperatures reached experimentally did not exceed 260 K [23, 24]:

$$\begin{aligned} \tau_{eff} &= \tau_{02D}\frac{E_F}{\hbar\omega}(1+\gamma') \\ \gamma' &= \frac{\tau_p}{2\tau_0}\frac{1}{q_0 L}\frac{1}{\left(E_F/\hbar\omega - 1/2\right)^{1/2}}. \end{aligned} \tag{11}$$

τ_{eff} in the degenerate case is calculated for a range of values of n_{2D} between 5.0×10^{12} cm^{-2} and 1.0×10^{14} cm^{-2}, and plotted in figure 9. At $n_{2D} = 1.5 \times 10^{13}$ cm^{-2}, which is the two-dimensional electron density in our sample, we obtain $\tau_{eff} \sim 0.7$ ps. This value is about two orders of magnitude higher than the electron–phonon scattering time constant τ_0 and is close to that calculated by Tsai *et al* [26]. In figure 10 we have plotted the energy relaxation rates versus inverse electron temperature using τ_{eff} values, obtained for both degenerate and non-degenerate statistics, in equation (7). We have also plotted the experimental power loss.

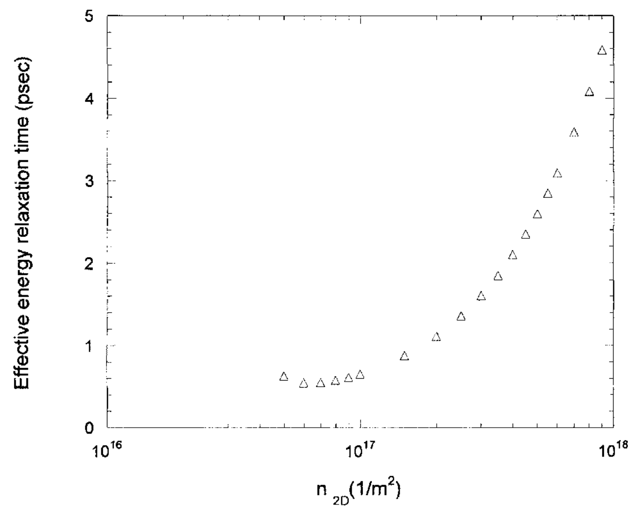

Figure 9. Effective energy relaxation time versus inverse electron temperature in the degenerate regime (equation (10)) at $T_L = 77$ K.

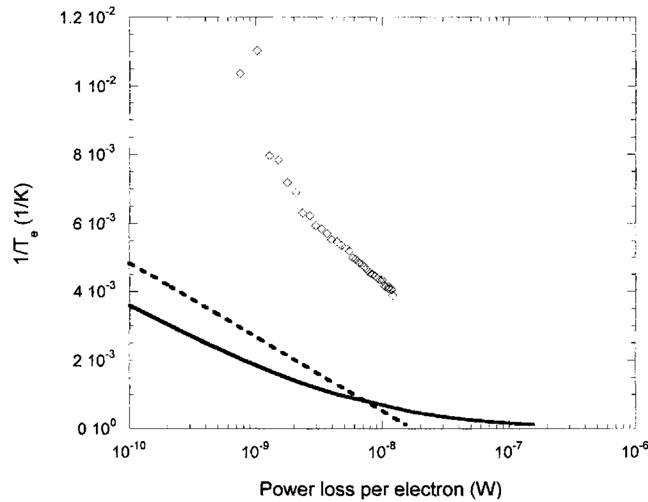

Figure 10. Experimental energy relaxation rates (squares) and theoretical rates assuming the production of hot phonons in the degenerate calculations (broken curve) and non-degenerate calculations (continuous curve) at $T_L = 77$ K.

It is clear from the figure that the experimental loss rates are significantly higher than either of the theoretical lines, in the range of measurements (although at high temperatures they tend to get closer). As we discussed above the reduced saturation drift velocity at high fields (plotted in figure 4) suggests strongly the presence of non-equilibrium phonons randomly distributed in the momentum space. Therefore, the reason for the observed disagreement between the experimental and the theoretical loss rates in figure 10 might be the failure of one of the other assumptions made in the mobility comparison method, or in the simplified theory. The theory, which is developed for an infinite GaAs quantum well, does not take into account of population of higher subbands at high fields, which is more likely to occur in a HEMT structure at the

GaN/AlGaN interface. Therefore, the assumption of a strong two-dimensional confinement of hot electrons made in the theory is questionable in the present case.

Furthermore, both the experimental and theoretical calculations for the steady state power loss are also based on the fundamental assumption that the e–e scattering results in the thermalization of the two-dimensional electrons, and hence the non-equilibrium electron gas can be represented by a statistical electron temperature, T_E. This assumption is true for an electron gas in GaAs quantum wells where the e–e scattering is about two orders of magnitude faster than the e–LO phonon scattering [27]. However, the accuracy of this assumption may need checking for a high-density two-dimensional gas at the GaN/AlGaN interface where, due to strong Frohlich coupling, the e–LO phonon scattering rates are comparable with the e–e scattering rates. The probable failure of the electron temperature model will also have implications in the accuracy of the hot-phonon model, where the non-equilibrium phonons are assumed to be represented by a statistical temperature (T_p) in thermal equilibrium with the hot electrons ($T_p = T_E$) [25].

3. Conclusions

We have studied the energy and momentum relaxation of a two-dimensional electron gas, which is formed at a GaN/AlGaN interface as a result of spontaneous and piezo-electric polarization, in the e–LO phonon scattering regime. We have shown that in the steady state drift velocity saturates at $v_d \sim 1.0 \times 10^7$ cm s^{-1} at an electric field of $E = 7500$ V cm^{-1} at $T_L = 77$ K, suggesting that the highest attainable drift velocity in the steady state is much smaller than those predicted by the existing theories. We have explained the observation in terms of the non-drifting hot-phonon model, which was developed and observed previously by us in highly modulation-doped GaAs quantum wells. Electron energy relaxation rates in GaN/AlGaN obtained from the mobility comparison method are compared with theoretical calculations based the assumption of on hot-phonon production (or otherwise) at high fields. We have not seen an agreement between the experimental results and the theory. Therefore, we expressed our concern about the accuracy of the electron temperature model for the non-equilibrium phonons and hence of the accuracy of the mobility comparison method. Experiments concerning the direct measurements of hot-electron distribution in the steady state (hot-electron photoluminescence) are underway and will be reported in the near future.

References

[1] Nakamura S and Fasol G 1997 *The Blue Laser Diode* (Berlin: Springer)
[2] Sheppard S T, Doverspike K, Pribble W L, Allen S T, Palmour J W, Kehias L T and Jenkins T J 1999 *IEEE Trans. Electron Devices Lett.* **20** 161
[3] Akasaki I and Amano H 1997 *Japan. J. Appl. Phys.* **36** 5293
[4] Harris J J *et al* 2001 *Semicond. Sci. Technol.* **16** 402
[5] Lee K J, Harris J J, Kent A J, Wang T, Sakai S, Maude D K and Portal J C 2001 *Appl. Phys. Lett.* **78** 2893
[6] Tsen K T, Ferry D K, Botchkarev A, Sverdlov B, Salvador A and Morkoc H 1997 *Appl. Phys. Lett.* **71** 1852
[7] Stanton N M, Kent A J, Akimov A V, Hawker P, Cheng T S and Foxon C T 2001 *J. Appl. Phys.* **89** 973
[8] Balkan N, Celik H, Cankurtaran M and Vickers A J 1995 *Phys. Rev.* B **52** 17 210
[9] Hess S, Walraet F, Taylor R A, Ryan J F, Beaumont B and Gibart P 1998 *Phys. Rev.* B **58** R15 973
[10] Stanton N M, Kent A J, Akimov A V, Hawker P, Cheng T S and Foxon C T 1999 *Phys. Status Solidi* a **176** 369
[11] Bulutay C, Ridley B K and Zakhleniuk N A 2000 *Appl. Phys. Lett.* **77** 2707
[12] Gelmont B, Kim K and Shur M 1993 *J. Appl. Phys.* **74** 1818
[13] Wraback M, Shen H, Carrano J C, Collins C J, Campbell J C, Dupuis R D, Schurman M J and Ferguson I T 2001 *Appl. Phys. Lett.* **79** 1303
[14] Ridley B K 2000 *Appl. Phys. Lett.* **77** 990

[15] Kane M J, Apsley N, Anderson D A, Taylor L L and Kerr T 1985 *J. Phys. C: Solid State Phys.* **18** 5629
[16] Ridley B K, Foutz B E and Eastman L F 2000 *Phys. Rev.* B **61** 16 862
[17] Ridley B K 1998 *J. Appl. Phys.* **84** 4020
[18] Dang X Z, Asbeck P M, Yu E T, Sullivan G J, Chen M Y, Mc Dermptt B T, Boutros K S and Redwing J M 1999 *Appl. Phys. Lett.* **74** 3890
[19] Gaska R, Shur M S, Bykhovski A D, Orlov A O and Snider G L 1999 *Appl. Phys. Lett.* **74** 287
[20] Oberhuber R, Zandler G and Vogl P 1998 *Appl. Phys. Lett.* **73**
[21] Mazzucato S, Arikan M C, Balkan N, Ridley B K, Zakhleniuk N, Shealy R J and Schaff B 2001 *Physica B* at press
[22] Foutz B E, O'Leary S K, Shur M S and Eastman L F 1999 *J. Appl. Phys.* **85** 7727
[23] Balkan N, Gupta R, Daniels M E, Ridley B K and Emeny M 1990 *Semicond. Sci. Technol.* **5** 986
[24] Gupta R, Balkan N and Ridley B K 1992 *Semicond. Sci. Technol.* B **7** 274
[25] Ridley B K 1989 *Semicond. Sci. Technol.* **4** 1142
[26] Tsai C-Y, Chen C-H, Sung T-Li, Tsai C-Y and Rorison J M 1999 *J. Appl. Phys.* **85** 1475
[27] Ridley B K 1988 *Quantum Processes in Semiconductors* (New York: Oxford University Press)